CRB1-associated retinal dystrophy patients have expanded Lewis glycoantigen-positive T cells

Moekotte, L.; Kuiper, J.J.W.; Hiddingh, S.; Nguyen, X.T.A.; Boon, C.J.F.; Born, L.I. van den; ... ; Genderen, M.M. van

CRB1-Associated Retinal Dystrophy Patients Have Expanded Lewis Glycoantigen-Positive T Cells

Lude Moekotte,[1] Jonas J. W. Kuiper,[1] Sanne Hiddingh,[1] Xuan-Thanh-An Nguyen,[2] Camiel J. F. Boon,[2,3] L. Ingeborgh van den Born,[4] Joke H. de Boer,[1] and Maria M. van Genderen[1,5]

[1]Department of Ophthalmology, University Medical Center Utrecht, Utrecht, the Netherlands
[2]Department of Ophthalmology, Leiden University Medical Center, Leiden, the Netherlands
[3]Department of Ophthalmology, Amsterdam University Medical Centers, Amsterdam, the Netherlands
[4]The Rotterdam Eye Hospital and Rotterdam Ophthalmic Institute, Rotterdam, the Netherlands
[5]Bartiméus, Diagnostic Center for complex visual disorders, Zeist, the Netherlands

Correspondence: Lude Moekotte, University Medical Center Utrecht, Heidelberglaan 100, Utrecht 3584 CX, the Netherlands; l.moekotte@umcutrecht.nl.

Received: March 24, 2023
Accepted: August 31, 2023
Published: October 4, 2023

Citation: Moekotte L, Kuiper JJW, Hiddingh S, et al. *CRB1*-associated retinal dystrophy patients have expanded lewis glycoantigen-positive T cells. *Invest Ophthalmol Vis Sci.* 2023;64(13):6. https://doi.org/10.1167/iovs.64.13.6

Purpose. Eye inflammation may occur in patients with inherited retinal dystrophies (IRDs) and is seen frequently in IRDs associated with mutations in the *CRB1* gene. The purpose of this study was to determine the types of inflammatory cells involved in IRDs, by deep profiling the composition of peripheral blood mononuclear cells of patients with a *CRB1*-associated IRD.

Methods. This study included 33 patients with an IRD with confirmed *CRB1* mutations and 32 healthy controls. A 43-parameter flow cytometry analysis was performed on peripheral blood mononuclear cells isolated from venous blood. FlowSOM and manual Boolean combination gating were used to identify and quantify immune cell subsets.

Results. Comparing patients with controls revealed a significant increase in patients in the abundance of circulating $CD4^+$ T cells and $CD8^+$ T cells that express sialyl Lewis X antigen. Furthermore, we detected a decrease in plasmacytoid dendritic cells and an $IgA^+CD24^+CD38^+$ transitional B-cell subset in patients with an IRD.

Conclusions. Patients with a *CRB1*-associated IRD show marked changes in blood leukocyte composition, affecting lymphocyte and dendritic cell populations. These results implicate inflammatory pathways in the disease manifestations of IRDs.

Keywords: inherited retinal dystrophy, *CRB1*, flow cytometry, inflammation

Inherited retinal dystrophies (IRDs) are a clinically and genetically heterogeneous group of monogenic diseases hallmarked by progressive loss of photoreceptors leading to severe visual impairment.[1–3] Among people of working age, IRDs are a leading cause of vision loss and blindness, which negatively impacts their quality of life.[4–6] To date, >270 genes are known to be associated with IRDs. Patients with identical gene mutations may have different clinical phenotypes and severity of disease, suggesting that other factors than genotype add to the disease mechanisms.[7]

The presence of elevated proinflammatory cytokines in the serum and eye fluid of patients implicate inflammatory responses in IRDs.[8–14] Patients with an IRDs show elevated serum levels of C-reactive protein, particularly those with the most significant vision loss.[15] Evidence of local cellular action against deteriorating eye tissues was demonstrated by the activation of microglia, T cells, and B cells in the eye fluid of patients.[16,17] Systemically, changes in peripheral blood monocytes[12] and dendritic cells (DCs) have been reported,[8] which may be harmful for the retina and may promote further progression of disease.[18,19] Furthermore, previous studies have reported the presence of systemic antiretinal antibodies in association with retinal disease and clinical manifestations.[20,21] Patients with RP with antiretinal antibodies demonstrated a more rapid deterioration of normalized visual field areas compared with those without antiretinal antibodies.[22] Collectively, these observations support the idea that inflammation worsens IRDs.

Inflammatory characteristics are particularly striking in patients with an IRD with mutations in the *Crumbs Homolog 1* (*CRB1*) gene, who in some cases may develop ocular inflammation masquerading as noninfectious uveitis.[7,8,10,23,24] Pathogenic mutations in the *CRB1* gene cause a phenotypical variety within the IRD spectrum, including RP, Leber congenital amaurosis, severe early childhood onset retinal dystrophy, and cone–rod dystrophies.[25,26] A variety of characteristics is associated with *CRB1*-associated IRDs, including early onset maculopathy, macular cysts, and increased retinal thickness with lamination.[27] The strong association with eye inflammation in *CRB1*-associated IRDs makes it an attractive phenotype for studying the role of immune mediators in this disease.

Quantification of circulating immune cell subsets may aid in better understanding the nature of these inflammatory responses. In this case control study, we investigated cell surface markers and intracellular markers of peripheral

blood mononuclear cells (PBMCs) through flow cytometry in patients with a *CRB1*-associated IRD.

Methods

Patients

This study was performed in compliance with the guidelines of the Declaration of Helsinki and had the approval of the local Institutional Review Board (University Medical Center Utrecht, [UMCU]). In total, 33 patients were referred to the UMCU from the Amsterdam University Medical Centers, Leiden University Medical Center, Bartiméus Diagnostic Center for complex visual disorders, The Rotterdam Eye Hospital and Rotterdam Ophthalmic Institute, and Groningen University Medical Center for recruitment at the outpatient clinic of the department of Ophthalmology of the UMCU (MEC-14-065). Patients had been diagnosed with IRD based on ophthalmic examination, imaging, and full-field ERG. Subsequent molecular genetic testing, either by targeted next-generation sequencing or by whole-exome sequencing, identified coding or deleterious mutations in the *CRB1* gene (Supplementary Table S4).

None of the patients had systemic inflammatory conditions at the time of sampling and/or received systemic immunomodulatory treatment. Ophthalmic examination took place at the day of inclusion, including visual acuity measurement and slit-lamp examination by an experienced uveitis specialist for the assessment of vitreous cells and vitreous haze.

We also included 32 anonymous blood donors at the UMCU with no history of ocular inflammatory disease who served as healthy controls. The mean age of patients and controls was 26.0 ± 15.6 years and 25.1 ± 8.8 years, respectively (Table 1).

Sample Processing

Blood was collected in lithium heparin vacutainers (#367874, BD Biosciences, Franklin Lakes, NJ, USA) through venipuncture, and PBMCs were isolated by Ficoll density gradient centrifugation (Supplementary Table S5). The PBMCs were then stored overnight in a Coolcell LX (#432002, Corning, Corning, NY, USA) at –80°C in 1:1 culture medium (10% fetal bovine serum, 8.9% Gibco RPMI Medium 1640 [#52400-025, Thermo Fisher Scientific, Waltham, MA, USA], and 1% penicillin-streptomycin) and freeze medium (80% fetal bovine serum and 20% dimethyl sulfoxide [#D5879-1L-M, Sigma-Aldrich, Munich, Germany]), after which they were stored in liquid nitrogen until measurement.

Staining of PBMCs

Samples were analyzed in 10 individual experiments across 2 periods between March 2021 (cohort 1) and November 2021 (cohort 2) (Fig. 1A). Samples were randomized for measurement in five experiments on individual measurement days. For each experiment, in total 6.5×10^6 thawed PBMCs were used, with varying number of samples (n) per panel owing to insufficient cells. We divided the cells over the following panels: B cell panel (5×10^5 cells; $n = 61$), conventional DC panel (2×10^6 cells; $n = 62$), mononuclear myeloid panel (2×10^6 cells; $n = 66$), a T helper panel with extracellular staining (5×10^5 cells; $n = 67$), and a T helper panel with intracellular staining (1.5×10^6 cells; $n = 65$) (Supplementary Table S1). After thawing and washing with PBS, 5% FcR Blocking Reagent (#130-059-901, Miltenyi Biotec, Bergisch Gladbach, Germany) was added to the PBMCs and incubated for 15 minutes at room temperature. For the intracellular panel, RPMI-1640 and Phorbol 12-myristate 13-acetate and Ionomycin solution were added and incubated at 37°C. After 30 minutes, BD GolgiStop (#51-2092KZ, BD Biosciences) was used to block intracellular transport protein processes and incubated for 3 hours at 37°C. Cells from each panel were then pipetted onto v-bottom wells plates and washed with PBS, after which 50 µL viability dye per well was added. After 10 minutes of incubation in the dark, the wells were washed with Dulbecco's PBS (#D8537-500ML, Sigma-Aldrich, Munich, Germany). Then the antibody mix specific for each panel (Supplementary Table S1) and Brilliant Stain Buffer (#563794, BD Biosciences) were added and incubated for 20 minutes at 4°C in the dark. For the intracellular panel, a Cytofix/Cytoperm Kit (#554714, BD Biosciences) was used to fixate and permeabilize the PBMCs, after which the intracellular antibody staining (Supplementary Table S1) was conducted for 20 minutes at 4°C. Finally, 300 µL fluorescent activated cell sorter buffer (Dulbecco's PBS, 1% Pharmingen-Stain Buffer [BSA], and 0.1% sodium azide) containing 100 µL precision count beads (#424902, Biolegend, San Diego, CA, USA) were added.

Flow Cytometry

The stained PBMCs were measured on the BD LSRFortessa Cell Analyzer (#647794, BD Biosciences) and compensated

Table 1. Study Population Demographics

	Cohort 1		Cohort 2		Total	
Demographics	Patient ($n = 15$)	Healthy Control ($n = 15$)	Patient ($n = 18$)	Healthy Control ($n = 17$)	Patient ($n = 33$)	Healthy Control ($n = 32$)
Female (%)	67% ($n = 10$)	47% ($n = 7$)	50% ($n = 9$)	59% ($n = 10$)	58% ($n = 19$)	53% ($n = 17$)
Age (years)	19.1 ± 6.5	26.3 ± 3.0	31.8 ± 18.5	24.0 ± 11.8	26.0 ± 15.6	25.1 ± 8.8
Clinical diagnosis						
RP	10 (67%)	–	13 (72%)	–	23 (70%)	–
LCA	5 (33%)	–	2 (11%)	–	7 (21%)	–
CRD	0 (0%)	–	2 (11%)	–	2 (6%)	–
MD	0 (0%)	–	1 (6%)	–	1 (3%)	–

CRD, cone–rod dystrophy; LCA, Leber congenital amaurosis; MD, macular dystrophy.

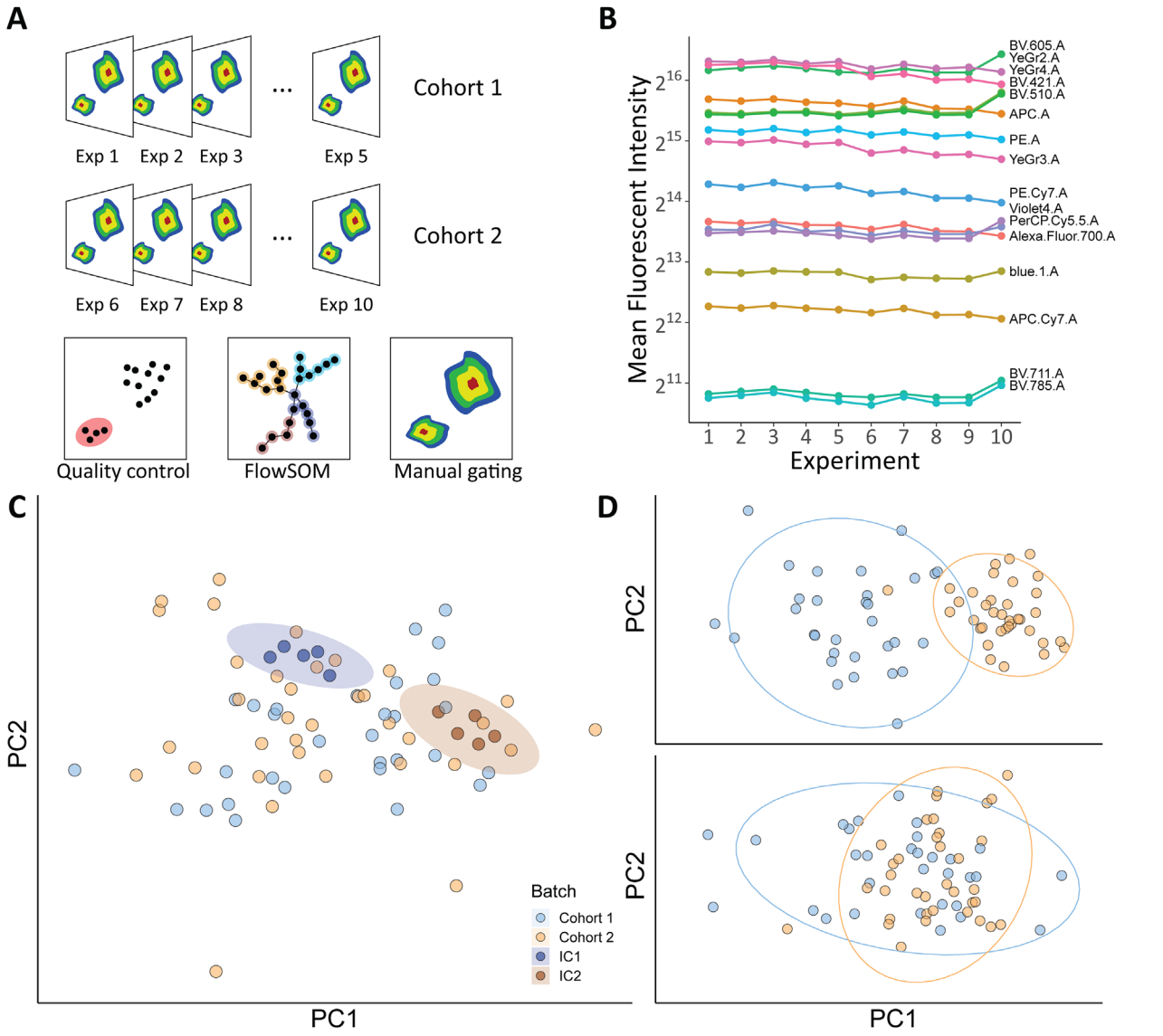

Figure 1. Study design and quality control. (**A**) The immune profiling was conducted by flow cytometry in frozen PBMCs of two cohorts of patients with a *CRB1*-associated IRDs and controls. After quality control, data from 10 flow cytometry experiments were combined for automatic gating by FlowSOM. The populations identified by FlowSOM were confirmed by manual gating. (**B**) Mean fluorescent intensities for (*rainbow*) calibration beads across the 10 experiments. The rainbow calibration beads demonstrated that the cytometry lasers performed consistently across multiple experiments. (**C**) The first two principal components of the manually gated data. The ellipse highlights the close cluster of the internal control samples used in the analysis of each cohort. (**D**) PCA of the median marker expression values (from flowSOM) before (*top*) and after (*bottom*) batch correction. Exp, experiment, IC, internal control.

in FACSDiva (BD Biosciences). Inter experimental variation was monitored by using PBMC aliquots of a single internal control in each experiment. Relative abundances were used for analyses.

Rainbow Calibration Beads (#422903, Biolegend) were used to measure the variance of the lasers of the flow cytometer between the measurement days, with stable results (Fig. 1B). The coefficient of variation was <10% across all individual channels. Before principal component analysis (PCA), missing data was imputed with the *missMDA* package, after which PCA was performed in R base on combined data of all experiments. This showed closely clustered internal controls of both cohort 1 and cohort 2, revealing high consistency in measurement days (Fig. 1C).

FlowSOM

After manually pregating compensated flow cytometry data in FlowJo (BD Biosciences) as shown in Supplementary Figure S1, all data from each experiment were transformed with the *estimateLogicle* function from the *flowCore* R package.[28] To improve power, data from all 10 experiments were combined with the *cyCombine* R package that adjusts for batch effects.[29] PCA within R base was performed on median

marker expression values before and after batch correction, and shows proper removal of batch effects (Fig. 1D). These data were then subjected to analysis by the *FlowSOM* R package, for which we used a 7 × 7 grid for all panels except for the conventional DC panel (8 × 8 grid).[30,31] The optimal number of metaclusters, cell clusters that are phenotypically similar, was determined by the elbow method, embedded in the *FlowSOM* R package. The results from the significant metaclusters were compared with frequency (%) of populations identified by standard manual gated data in FlowJo (version 10.8.1) as shown in Supplementary Figures S1 and S3.

Statistical Analyses

All statistical analyses were performed in R and R studio (version 4.2.2). To compare the abundance of cells in each metacluster between patients and healthy controls, missing data was imputed with the *missMDA* package and a likelihood-ratio test (using age and sex as covariates in the models) was performed. The *P* values were adjusted using the Benjamini–Hochberg procedure with the *p.adjust* function in R base. An adjusted *P* value (P_{adj}) of <0.05 was considered statistically significant. Scatter plots for the interpretation of the data were made within the *ggplot2* R package.

Results

We analyzed cellular subsets in peripheral blood of 33 patients and 32 controls by flow cytometry in 2 large cohorts of in total 10 individual experiments (Fig. 1A). We ascertained high quality of our data as shown by the consistent technical performance across the experiments (Figs. 1B–D).

Next, we subjected the flow cytometry data to analysis by FlowSOM. FlowSOM considers the total profile of expressed surface markers for hierarchical clustering of cells to allow unbiased (immune) cell identification. FlowSOM spanning trees for each flow cytometry panel are detailed in Supplementary Figure S2. In total, the abundance of 10 metaclusters differed significantly ($P_{adj} < 0.05$) between patients with an IRD and controls (heatmap in Fig. 2 and Supplementary Table S2), which we verified by manual gating (Supplementary Fig. S3 and Supplementary Table S3A–C). In detail, we observed a skewing towards $CD4^+CD45RO^+$ effector memory T cells in patients with a *CRB1*-IRDs (metacluster *Th7*; $P = 0.0017$). Several changes in distinct functional T-cell populations were identified, such as $CD4^+$ T cells that express an epitope of the sialyl Lewis X antigen (also known as cutaneous lymphocyte-associated antigen), which were increased in abundance in blood of patients (metaclusters *Tskew1*, $P = 0.0015$, and *Tskew6*, $P < 0.001$) (Fig. 3). Interestingly, an expansion of T cells positive for this tissue-homing marker was also observed in cytotoxic $CD8^+$ T cells (metacluster *Tskew3*, $P < 0.001$) (Fig. 3).

In $CD8^+$ T cells, we further noted an increased abundance of $CD8^+$ T cells expressing another tissue-homing marker, the *Integrin alpha E* also known as CD103 (metacluster *Th3*, $P < 0.001$). Collectively, these data support that circulating T cells expressing tissue-homing markers are expanded in patients with an IRDs.

Analyses using panels targeting myeloid mononuclear cell populations identified a significant decrease in $CD303^+CD123^+$ plasmacytoid DCs (pDCs) (metacluster *DCm7*, $P = 0.0029$) (Fig. 4). Additionally, data from the cDC panel independently supported a significant decrease in pDCs. Despite the lack of pDC-specific markers in this panel, a metacluster of $HLA\text{-}DR^+Lin^-CD11c^-CD36^+CCR2^+$ cells (representing pDCs) were significantly decreased (*cDC3*, $P = 0.0040$) and highly correlated with the $CD303^+CD123^+$

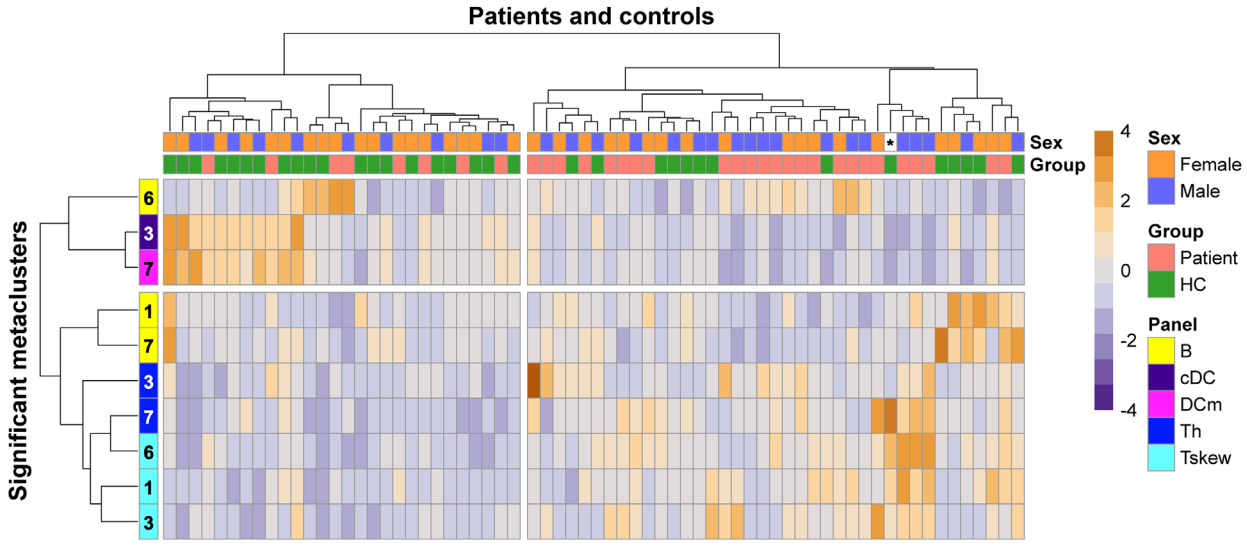

Figure 2. FlowSOM metaclusters with significant changes. Heatmap of unsupervised clustering of all statistically significant ($P_{adj} < 0.05$) FlowSOM metaclusters identified in this study, divided in four based on hierarchical clustering for visualization purposes. Heatmap colors represent the changes in proportion from a relatively low proportion (in *purple blue*) to a higher proportion (in *dark orange*). Dendrograms indicating the clustering relationships (Euclidean distance and Ward2's method) between disease groups and leukocyte populations are shown to the left and above the heatmap. Sex of one control, indicated by an asterisk (*), is missing. A higher proportion of T cells and a lower proportion of B cells and dendritic cells in patients can be appreciated. cDC, conventional dendritic cell panel; DCm, dendritic cell mononuclear panel; HC, healthy control; Th, T helper panel with extracellular staining; Tskew, T helper panel with intracellular staining.

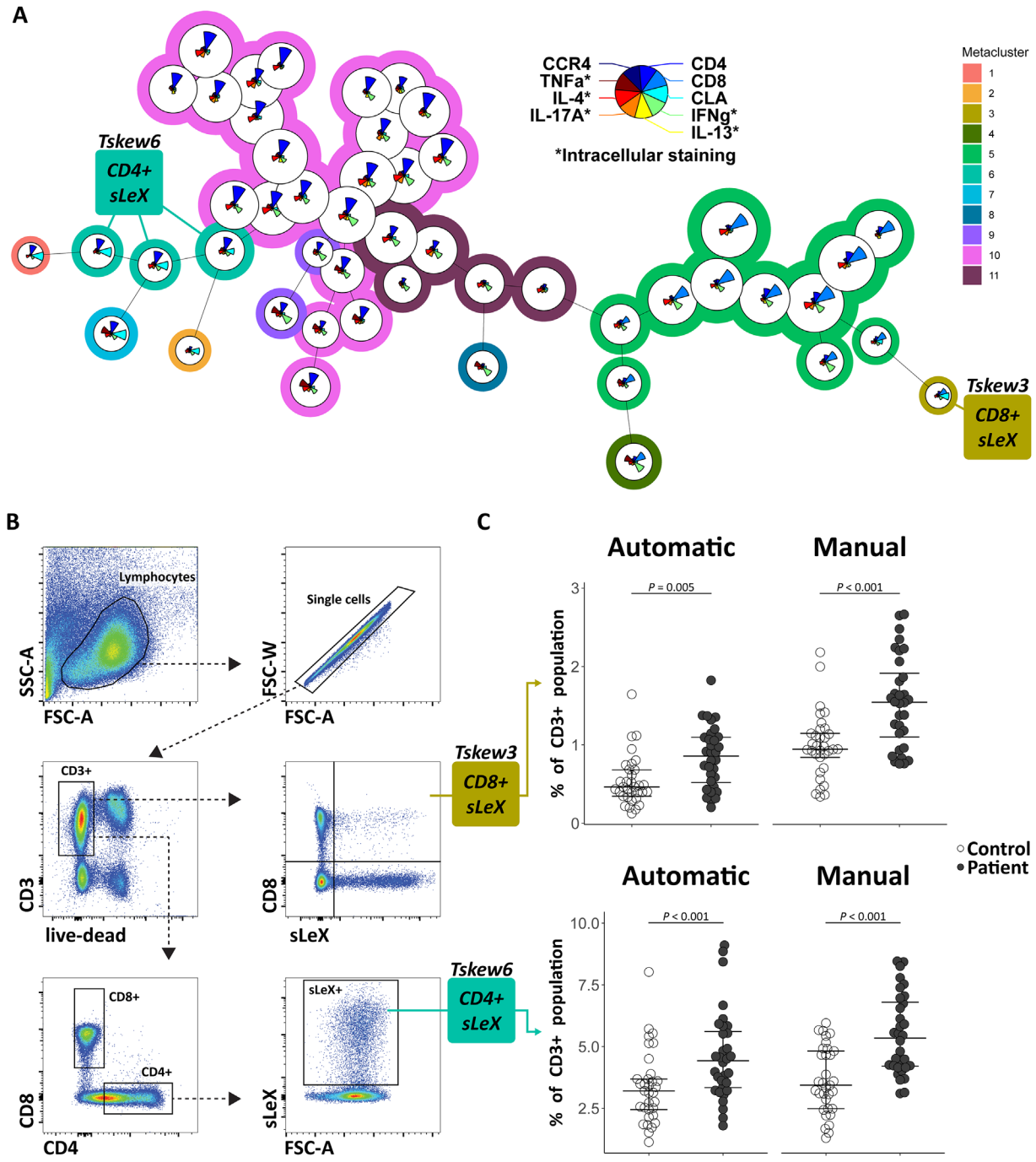

Figure 3. *CRB1*-associated IRDs are characterized by an increase in Lewis Antigen-positive T cells. (**A**) The FlowSOM tree for the T helper cell panel in patients and controls (combined). Metaclusters of $CD8^+$ and $CD4^+$ T cells expressing the sialyl Lewis X Antigen/CLA epitope are highlighted. The size of the pie chart is relative to the cluster size (ie, median percentage cells in the $CD3^+$ gate). The star charts visualize the relative surface/intracellular marker expression used to distinguish the clusters. Metacluster colors are shown as background color of the clusters. (**B**) The manual gating strategy to identify the significant populations found in the FlowSOM tree. (**C**) The abundance of cells in patients and controls. Benjamini–Hochberg post hoc adjusted *P* values are from the likelihood-ratio test corrected for age and sex. Median and interquartile range are indicated by bars. CCR4, CC chemokine receptor type 4; CD, cluster of differentiation; CLA, cutaneous lymphocyte antigen; IFNg, interferon gamma; IL, interleukin; sLeX, sialyl Lewis X antigen; TNF-a, tumor necrosis factor alpha.

metacluster in the DCm panel (Pearson correlation, r = 0.96, $P < 0.001$).

Finally, we observed a decrease in frequency of B cells double positive for IgA and *CD24* (also called Heat Stable Antigen or nectadrin) (metacluster *B7*, $P < 0.001$) and IgG^+CD27^+ B cells (metacluster *B1*, $P = 0.0075$). Another metacluster (*B6*) was increased in patients, but this metacluster comprised of mixed populations ($IgM^{+/-}$, $CD24^{+/-}$, and $CD38^{+/-}$), which hampered confirmation by manual gating.

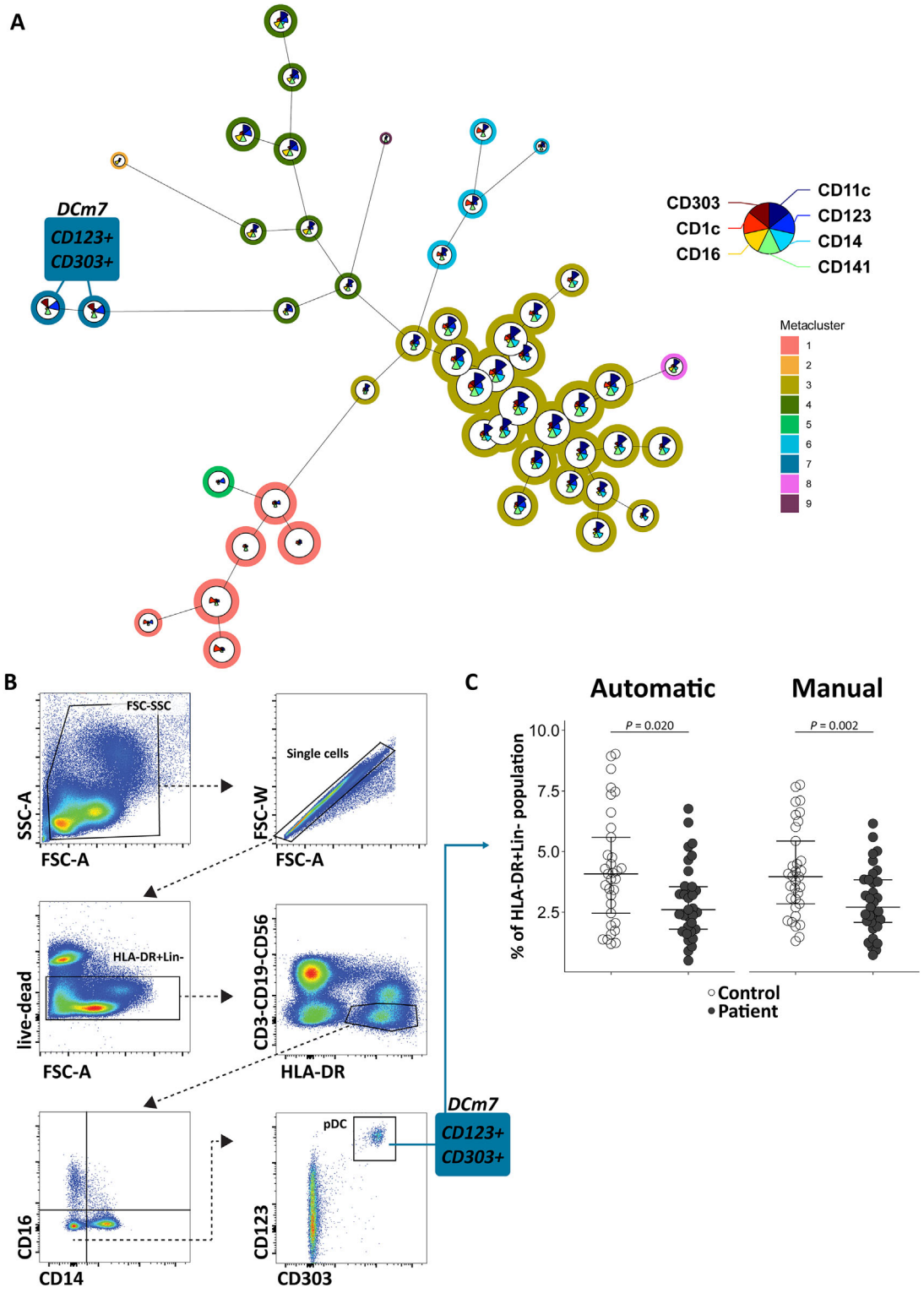

Figure 4. pDCs are decreased in *CRB1*-associated IRDs. (**A**) The FlowSOM tree for the mononuclear myeloid panel in patients and controls (combined). Metacluster of pDCs is highlighted. The size of the pie chart is relative to the cluster size (ie, median percentage cells in the HLA-DR^{+}Lin^{-} gate). The star charts visualize the relative surface marker expression used to distinguish the clusters. Metacluster colors are shown as background color of the clusters. (**B**) The manual gating strategy to identify the significant populations found in the FlowSOM tree. (**C**) The abundance of cells in patients and controls. Benjamini–Hochberg post hoc adjusted *P* values are from the likelihood ratio test corrected for age and sex. Median and interquartile range are indicated by bars. CD, cluster of differentiation.

Discussion

Using deep immunophenotyping, we identified a significant expansion of blood T-cell populations expressing tissue-homing markers, as well as a decrease in circulating pDCs, in patients with a *CRB1*-associated IRD.

The pathogenesis of IRDs is thought to be influenced by chronic reactive inflammation, because patients often manifest vitreous cells, show elevated inflammatory cytokine levels in eye fluid,[32] and the improvement of retinal function upon treatment with systemic immunomodulating treatment agents.[33] Studies dating back to the early 1980s have shown T-cell reactivity to retinal antigens in patients with an IRDs.[34,35]

Direct involvement of T cells in *CRB1*-associated IRDs requires their access to the ocular microenvironment which is orchestrated by "migratory" receptors that function by targeting ligands with relative spatial and tissue-specific expression patterns (so-called homing of T cells). Our findings show the expansion of specialized subsets of cytotoxic and T helper populations that express tissue-migration markers, such as sialyl Lewis X determinant/cutaneous lymphocyte-associated antigen and CD103. The tissue-homing integrin CD103 is expressed at high levels on T cells found at tissue barriers, including the skin, eyes, and the mucosa of the gut.[36] This link between $CD103^+$ T cells and the gut is of interest because IRDs exhibit shifts in the composition of the gut microbiome, and gut dysbiosis exacerbates retinal degeneration in IRD models by promoting inflammatory-related pathways.[37,38] Furthermore, CD103 has been reported to be increased in uveitis.[39,40] Functionally, CD103 binds to the epithelial cell marker E-cadherin and is upregulated upon exposure to immunomodulatory cytokines, such as TGF-β. The CD103 receptor is well-expressed by corneal-resident T cells,[41] as well as by retinal-resident T cells under inflammatory conditions.[40]

To understand the implications of sialyl Lewis X determinant on T cells in IRDs, we need to consider some properties of this antigen. We probed the sialyl Lewis X determinant with the HECA-452 antibody, which has been shown to react to a complex mixture of Lewis X glycoconjugates, predominantly a specific epitope of the sialyl Lewis X determinant termed "sialyl 6-sulfo Lewis X."[42,43] As this epitope is primarily studied on skin-homing T lymphocytes, it is also known as "cutaneous lymphocyte-associated antigen," which is known to play an important role in lymphocyte homing.[44,45] Possibly, there are differences between $CD4^+$ and $CD8^+$ T cells in the precise determinant of Lewis X antigen recognized in our studies of IRDs. Sialyl 6-sulfo Lewis X is more restricted to $CD4^+$ T cells, whereas $CD8^+$ T cells may express the "classical" Lewis X antigen. Regardless, these Lewis X determinants serve as a ligand for E-, P-, and L-selectins[46–48] and aid in the extravasation of leukocytes,[49,50] as well as in the inflamed eye.[51] Further studies to determine the function of the Lewis glycoprotein-positive T cells in the context of IRDs are required to determine if these T cells are antigen specific and/or proinflammatory or regulatory in nature. Regardless, the expansion of tissue-migration receptors by helper and cytotoxic T cells emphasizes the active involvement of T cells in this group of IRDs.

Another key observation from our study is a significant decrease in pDC abundance in patients. This finding is of interest, because a decrease in pDCs is also a characteristic finding in studies of chronic inflammatory conditions, such as noninfectious uveitis, systemic lupus erythematosus, and various types of cancer.[52–55] PDCs are antigen-presenting cells best known for their key role in antiviral immunity.[56] Indeed, pDCs have the capability of producing large amounts of type I IFN upon recognizing either viral or endogenous RNA/DNA.[57–59] We previously showed that type I IFNs are elevated in *CRB1*-associated IRDs masquerading as intraocular inflammation.[8] We would like to stress that the bulk of research on pDCs is focused on type I IFN signaling, whereas many other functions of these cells remain underexplored. For instance, pDCs are found in the retina and other eye tissues and may respond to tissue injury in the eye by producing antiangiogenic factors that inhibit neovascularization.[60] However, little is known about the function of pDCs in retinal disease, and research should focus on the vast array of other functional receptors of these cells that are involved in a variety of regulatory and inflammatory functions, such as CD36 (detected in our study). The scavenger receptor CD36 binds apoptotic cell debris[61–63] and is involved in photoreceptor degeneration and retinal inflammation in murine models.[64,65] CD5L, a binding partner of CD36, is also found to be expressed in the RPE,[66–69] as well as in resident microglial cells.[66] Autoimmunity in AMD is suggested through anti-CD5L autoreactivity, implicating CD5L in retinal pathogenesis. Although the decrease in circulating pDCs could reflect in part their infiltration into peripheral tissues, note that we identified pDCs using CD303 and CD123 surface markers. CD123 (or IL-3R-A) expression may decrease in inflammatory states when pDCs are lost from circulation by cell death.[70] In contrast, activation of pDCs by triggering CD303 signaling in pDCs leads to internalization of this lectin receptor (lower expression among pDCs),[71] which has been demonstrated in in vitro culture of pDCs.[72] Perhaps this finding is also true for the decreasing number of $HLA^-DR^+CD11c^-CD36^+$ pDCs in patients with an IRD, because CD36 also decreases after pDC activation.[73] Regardless, these observations implicate pDCs in IRDs and provide new clues in our understanding of the cell types involved.

Other observations of interest concern the IgA^+CD24^+ and IgG^+CD27^+ B cells. This result might implicate involvement of the humoral immune response in IRDs. This finding is of interest because retinal autoantibodies have been reported in IRDs, most notably in patients presenting with cystoid macular edema,[20,21,35,74,75] a comorbidity associated with *CRB1* mutations.[76]

Results should be interpreted with consideration of the study's limitations. IRDs affect approximately 1 in every 2000 to 3000 individuals, of which mutations in the *CRB1* gene are detected in approximately 5% of cases.[77–81] Because of the rarity of the disease, the sample size was relatively small, limiting statistical power to assess differences between phenotypes or further stratification of patients based on clinical characteristics. The latter was also complicated by lack of standardization of disease activity in *CRB1*-associated IRDs, and the already mentioned variation in disease course. We did not have access to additional ophthalmic examinations, such as fluorescein angiography and optical coherence tomography, possibly missing the full breadth of inflammatory implications in the eye. An exciting opportunity for a follow-up study would be to prospectively investigate patients from onset of disease, to determine the dynamics of blood leukocyte populations and their relation with disease progression based on clinical findings (e.g., visual field progression and imaging). Although ocular inflammation can be found in many types of IRDs, we limited our study to those with confirmed *CRB1* mutations, because of the

Investigative Ophthalmology & Visual Science

high occurrence of CME in these patients, which is strongly associated with inflammation.[8,10,76] We showed that this inflammation exhibits striking similarities to other inflammatory eye conditions, in which T cells and pDCs are also implicated.[52] These findings make it tempting to speculate that anti-inflammatory agents might be able to slow down disease progression in people with *CRB1*-associated IRDs,[8] and although murine studies have shown a neuroprotective effect of immunosuppressants, further research is needed to determine whether this outcome also applies to other types of IRDs in human patients.[33,82] The number of markers used for immunophenotyping in our work is not exhaustive and was preselected owing to the spectral limitations of flow cytometry. Furthermore, our study followed a snapshot approach, which brings limitations owing to changes in the immune profile throughout time. To better understand the landscape of T cells associated with *CRB1*-associated IRDs, we recommend further (prospective) studies by expanding flow cytometry analysis with other T-cell–specific markers, or by using unbiased sequencing approaches (e.g., *CITE*-seq). Ideally, such studies include ocular fluid biopsies from patients to probe the ocular microenvironment of IRDs. Additionally, autoantibody testing could prove useful in future screening in patients with an IRD.

In conclusion, we demonstrated that *CRB1*-associated IRDs are characterized by substantial changes in the peripheral T cells and DC compartments and suggest that interventions that suppress ocular inflammatory reactions, as shown promising in previous studies,[33,83,84] should be explored as a potential disease-modifying intervention.

Acknowledgments

The authors thank N.H. ten Dam-van Loon, J. Ossewaarde-van Norel, and V. Koopman-Kalinina Ayuso for their assistance performing slit-lamp examinations and assessment of vitreous cells and vitreous haze on all included patients.

Funding: Bartiméus Fonds.

Disclosure: **L. Moekotte**, None; **J.J.W. Kuiper**, None; **S. Hiddingh**, None; **X.-T.-A. Nguyen**, None; **C.J.F. Boon**, None; **L.I. van den Born**, None; **J.H. de Boer**, None; **M.M. van Genderen**, None

References

1. Verbakel SK, van Huet RAC, Boon CJF, et al. Non-syndromic retinitis pigmentosa. *Prog Retin Eye Res*. 2018;66:157–186.
2. Hartong DT, Berson EL, Dryja TP. Retinitis pigmentosa. *Lancet*. 2006;368(9549):1795–1809.
3. Hamel C. Retinitis pigmentosa. *Orphanet J Rare Dis*. 2006; 1(1):40.
4. Heath Jeffery RC, Mukhtar SA, McAllister IL, Morgan WH, Mackey DA, Chen FK. Inherited retinal diseases are the most common cause of blindness in the working-age population in Australia. *Ophthalmic Genet*. 2021;42(4):431–439.
5. Liew G, Michaelides M, Bunce C. A comparison of the causes of blindness certifications in England and Wales in working age adults (16-64 years), 1999-2000 with 2009-2010. *BMJ Open*. 2014;4(2):e004015.
6. Erratum: vision-related quality of life in patients with inherited retinal dystrophies. *J Curr Ophthalmol*. 2022;34(3):387.
7. Bujakowska K, Audo I, Mohand-Säid S, et al. CRB1 mutations in inherited retinal dystrophies. *Hum Mutat*. 2012;33(2):306.
8. Verhagen F, Kuiper J, Nierkens S, Imhof SM, Radstake T, de Boer J. Systemic inflammatory immune signatures in a patient with CRB1 linked retinal dystrophy. *Expert Rev Clin Immunol*. 2016;12(12):1359–1362.
9. Alves CH, Wijnholds J. Microglial cell dysfunction in CRB1-associated retinopathies. *Adv Exp Med Biol*. 2019;1185:159–163.
10. Hettinga YM, van Genderen MM, Wieringa W, Ossewaarde-van Norel J, de Boer JH. Retinal dystrophy in 6 young patients who presented with intermediate uveitis. *Ophthalmology*. 2016;123(9):2043–2046.
11. Yoshida N, Ikeda Y, Notomi S, et al. Clinical evidence of sustained chronic inflammatory reaction in retinitis pigmentosa. *Ophthalmology*. 2013;120(1):100–105.
12. Mohan KV, Mishra A, Muniyasamy A, et al. Immunological consequences of compromised ocular immune privilege accelerate retinal degeneration in retinitis pigmentosa. *Orphanet J Rare Dis*. 2022;17(1):378.
13. Okita A, Murakami Y, Shimokawa S, et al. Changes of serum inflammatory molecules and their relationships with visual function in retinitis pigmentosa. *Invest Ophthalmol Vis Sci*. 2020;61(11):30.
14. Lu B, Yin H, Tang Q, et al. Multiple cytokine analyses of aqueous humor from the patients with retinitis pigmentosa. *Cytokine*. 2020;127:154943.
15. Murakami Y, Ikeda Y, Nakatake S, et al. C-Reactive protein and progression of vision loss in retinitis pigmentosa. *Acta Ophthalmol*. 2018;96(2):e174–e179.
16. Newsome DA, Michels RG. Detection of lymphocytes in the vitreous gel of patients with retinitis pigmentosa. *Am J Ophthalmol*. 1988;105(6):596–602.
17. Gupta N, Brown KE, Milam AH. Activated microglia in human retinitis pigmentosa, late-onset retinal degeneration, and age-related macular degeneration. *Exp Eye Res*. 2003;76(4):463–471.
18. Sun Y, Lin Z, Liu CH, et al. Inflammatory signals from photoreceptor modulate pathological retinal angiogenesis via c-Fos. *J Exp Med*. 2017;214(6):1753–1767.
19. Massengill MT, Ahmed CM, Lewin AS, Ildefonso CJ. Neuroinflammation in retinitis pigmentosa, diabetic retinopathy, and age-related macular degeneration: a minireview. *Adv Exp Med Biol*. 2018;1074:185–191.
20. Heckenlively JR, Solish AM, Chant SM, Meyers-Elliott RH. Autoimmunity in hereditary retinal degenerations. II. Clinical studies: antiretinal antibodies and fluorescein angiogram findings. *Br J Ophthalmol*. 1985;69(10):758–764.
21. Heckenlively JR, Jordan BL, Aptsiauri N. Association of antiretinal antibodies and cystoid macular edema in patients with retinitis pigmentosa. *Am J Ophthalmol*. 1999;127(5):565–573.
22. Heckenlively JR, Aptsiauri N, Nusinowitz S, et al. Investigations of antiretinal antibodies in pigmentary retinopathy and other retinal degenerations. *Trans Am Ophthalmol Soc*. 1996;94:179. Accessed July 13, 2023, https://www.ncbi.nlm.nih.gov/pmc/articles/PMC1312095/.
23. Watson CM, El-Asrag M, Parry DA, et al. Mutation screening of retinal dystrophy patients by targeted capture from tagged pooled DNAs and next generation sequencing. *PLoS One*. 2014;9(8):e104281.
24. De Castro-Miró M, Pomares E, Lorés-Motta L, et al. Combined genetic and high-throughput strategies for molecular diagnosis of inherited retinal dystrophies. *PLoS One*. 2014;9(2):e88410.
25. Talib M, van Schooneveld MJ, van Genderen MM, et al. Genotypic and phenotypic characteristics of CRB1-associated retinal dystrophies: a long-term follow-up study. *Ophthalmology*. 2017;124(6):884–895.

26. Zahid S, Branham K, Schlegel D, et al. CRB1. In: *Retinal Dystrophy Gene Atlas*. New York: Springer International Publishing; 2018:75–78.
27. Khan KN, Robson A, Mahroo OAR, et al. A clinical and molecular characterisation of CRB1-associated maculopathy. *Eur J Hum Genet*. 2018;26(5):687–694.
28. Hahne F, LeMeur N, Brinkman RR, et al. flowCore: a Bioconductor package for high throughput flow cytometry. *BMC Bioinformatics*. 2009;10:145.
29. Pedersen CB, Dam SH, Barnkob MB, et al. cyCombine allows for robust integration of single-cell cytometry datasets within and across technologies. *Nat Commun*. 2022;13(1):1698.
30. Van Gassen S, Callebaut B, Van Helden MJ, et al. FlowSOM: using self-organizing maps for visualization and interpretation of cytometry data. *Cytometry A*. 2015;87(7):636–645.
31. Quintelier K, Couckuyt A, Emmaneel A, Aerts J, Saeys Y, Van Gassen S. Analyzing high-dimensional cytometry data using FlowSOM. *Nat Protoc*. 2021;16(8):3775–3801.
32. Kanski JJ. Retinitis Pigmentosa. In: *Clinical Ophthalmology: A Systematic Approach*. 6th ed. Oxford, UK: Pergamon Press; 2009.
33. Sarici K, Vyas A, Iannaccone A. The double-edged sword of inflammation in inherited retinal degenerations: clinical and preclinical evidence for mechanistically and prognostically impactful but treatable complications. *Front Cell Dev Biol*. 2023;11:177711.
34. Kumar M, Gupta RM, Nema H V. Role of autoimmunity in retinitis pigmentosa. *Ann Ophthalmol*. 1983;15(9):838–840, Accessed February 21, 2023. https://europepmc.org/article/med/6607015.
35. Chant SM, Heckenlively J, Meyers-Elliott RH. Autoimmunity in hereditary retinal degeneration. I. Basic studies. *Br J Ophthalmol*. 1985;69(1):19–24.
36. Sathaliyawala T, Kubota M, Yudanin N, et al. Distribution and compartmentalization of human circulating and tissue-resident memory T cell subsets. *Immunity*. 2013;38(1):187–197.
37. Kutsyr O, Maestre-Carballa L, Lluesma-Gomez M, Martinez-Garcia M, Cuenca N, Lax P. Retinitis pigmentosa is associated with shifts in the gut microbiome. *Sci Rep*. 2021;11(1):6692.
38. Kutsyr O, Noailles A, Martínez-Gil N, et al. Short-term high-fat feeding exacerbates degeneration in retinitis pigmentosa by promoting retinal oxidative stress and inflammation. *Proc Natl Acad Sci USA*. 2021;118(43):e2100566118.
39. Robles-Contreras A, Groman-Lupa S, Pedroza-Seres M, De Lucio VB, Garfias Y, Martinez MCJ. Uveitis ocular damage could be associated with increased frequency of CD8+CD57+CD103+CD108+ cells. *Invest Ophthalmol Vis Sci*. 2010;51(13):4848–4848.
40. Boldison J, Chu CJ, Copland DA, et al. Tissue-resident exhausted effector memory CD8+ T cells accumulate in the retina during chronic experimental autoimmune uveoretinitis. *J Immunol*. 2014;192(10):4541–4550.
41. Loi JK, Alexandre YO, Senthil K, et al. Corneal tissue-resident memory T cells form a unique immune compartment at the ocular surface. *Cell Rep*. 2022;39(8):110852.
42. Ohmori K, Fukui F, Kiso M, et al. Identification of cutaneous lymphocyte-associated antigen as sialyl 6-sulfo Lewis X, a selectin ligand expressed on a subset of skin-homing helper memory T cells. *Blood*. 2006;107(8):3197–3204.
43. Kannagi R, Ohmori K, Kimura N. Anti-oligosaccharide antibodies as tools for studying sulfated sialoglycoconjugate ligands for siglecs and selectins. *Glycoconj J*. 2009;26(8):923–928.
44. Yoshino T, Okano M, Chen HL, et al. Cutaneous lymphocyte antigen is expressed on memory/effector B cells in the peripheral blood and monocytoid B cells in the lymphoid tissues. *Cell Immunol*. 1999;197(1):39–45.
45. Rossiter H, Van Reijsen F, Mudde GC, et al. Skin disease-related T cells bind to endothelial selectins: expression of cutaneous lymphocyte antigen (CLA) predicts E-selectin but not P-selectin binding. *Eur J Immunol*. 1994;24(1):205–210.
46. Ohmori K, Kanda K, Mitsuoka C, et al. P- and E-selectins recognize sialyl 6-sulfo Lewis X, the recently identified L-selectin ligand. *Biochem Biophys Res Commun*. 2000;278(1):90–96.
47. Yoshino K, Ohmoto H, Kondo N, et al. Studies on selectin blockers. 4. Structure-function relationships of sulfated sialyl Lewis X hexasaccharide ceramides toward E-, P-, and L-selectin binding. *J Med Chem*. 1997;40(4):455–462.
48. Kanamori A, Kojima N, Uchimura K, et al. Distinct sulfation requirements of selectins disclosed using cells that support rolling mediated by all three selectins under shear flow. L-selectin prefers carbohydrate 6-sulfation totyrosine sulfation, whereas p-selectin does not. *J Biol Chem*. 2002;277(36):32578–32586.
49. Milstone DS, O'Donnell PE, Stavrakis G, Mortensen RM, Davis VM. E-selectin expression and stimulation by inflammatory mediators are developmentally regulated during embryogenesis. *Lab Invest*. 2000;80(6):943–954.
50. Santamaria Babi LF, Perez Soler MT, Hauser C, Blaser K. Skin-homing T cells in human cutaneous allergic inflammation. *Immunol Res*. 1995;14(4):317–324.
51. Suzuma I, Mandai M, Suzuma K, Ishida K, Tojo SJ, Honda Y. Contribution of E-selectin to cellular infiltration during endotoxin-induced uveitis. *Invest Ophthalmol Vis Sci*. 1998;39(9):1620–1630.
52. Verhagen FH, Hiddingh S, Rijken R, et al. High-dimensional profiling reveals heterogeneity of the Th17 subset and its association with systemic immunomodulatory treatment in non-infectious uveitis. *Front Immunol*. 2018;9:2519.
53. Tucci M, Quatraro C, Lombardi L, Pellegrino C, Dammacco F, Silvestris F. Glomerular accumulation of plasmacytoid dendritic cells in active lupus nephritis: role of interleukin-18. *Arthritis Rheum*. 2008;58(1):251–262.
54. Fiore N, Castellano G, Blasi A, et al. Immature myeloid and plasmacytoid dendritic cells infiltrate renal tubulointerstitium in patients with lupus nephritis. *Mol Immunol*. 2008;45(1):259–265.
55. Greene TT, ra Jo Y, Zuniga EI. Infection and cancer suppress pDC derived IFN-I. *Curr Opin Immunol*. 2020;66:114–122.
56. Tang F, Du Q, Liu YJ. Plasmacytoid dendritic cells in antiviral immunity and autoimmunity. *Sci China Life Sci*. 2010;53(2):172–182.
57. Alculumbre S, Raieli S, Hoffmann C, Chelbi R, Danlos FX, Soumelis V. Plasmacytoid pre-dendritic cells (pDC): from molecular pathways to function and disease association. *Semin Cell Dev Biol*. 2019;86:24–35.
58. Wimmers F, Subedi N, van Buuringen N, et al. Single-cell analysis reveals that stochasticity and paracrine signaling control interferon-alpha production by plasmacytoid dendritic cells. *Nat Commun*. 2018;9(1):3317.
59. Musumeci A, Lutz K, Winheim E, Krug AB. What makes a pDC: recent advances in understanding plasmacytoid DC development and heterogeneity. *Front Immunol*. 2019;10(MAY):1222.
60. Jamali A, Kenyon B, Ortiz G, et al. Plasmacytoid dendritic cells in the eye. *Prog Retin Eye Res*. 2021;80:100877.
61. Albert ML, Pearce SFA, Francisco LM, et al. Immature dendritic cells phagocytose apoptotic cells via alphavbeta5 and CD36, and cross-present antigens to cytotoxic T lymphocytes. *J Exp Med*. 1998;188(7):1359–1368.
62. Böttcher A, Gaipl US, Fürnrohr BG, et al. Involvement of phosphatidylserine, alphavbeta3, CD14, CD36, and comple-

Investigative Ophthalmology & Visual Science

ment C1q in the phagocytosis of primary necrotic lymphocytes by macrophages. *Arthritis Rheum*. 2006;54(3):927–938.
63. Sharma P, Tseng HH, Lee JYL, Tsai EM, Suen JL. A prominent environmental endocrine disruptor, 4-nonylphenol, promotes endometriosis development via plasmacytoid dendritic cells. *Mol Hum Reprod*. 2020;26(8):601–614.
64. Lavalette S, Conart JB, Touhami S, et al. CD36 deficiency inhibits retinal inflammation and retinal degeneration in Cx3cr1 knockout mice. *Front Immunol*. 2020;10:3032.
65. Mellal K, Omri S, Mulumba M, et al. Immunometabolic modulation of retinal inflammation by CD36 ligand. *Sci Rep*. 2019;9(1):12903.
66. Iannaccone A, Hollingsworth TJ, Koirala D, et al. Retinal pigment epithelium and microglia express the CD5 antigen-like protein, a novel autoantigen in age-related macular degeneration. *Exp Eye Res*. 2017;155:64–74.
67. Ryeom SW, Sparrow JR, Silverstein RL. CD36 participates in the phagocytosis of rod outer segments by retinal pigment epithelium. *J Cell Sci*. 1996;109(Pt 2):387–395.
68. Kauppinen A, Niskanen H, Suuronen T, Kinnunen K, Salminen A, Kaarniranta K. Oxidative stress activates NLRP3 inflammasomes in ARPE-19 cells–implications for age-related macular degeneration (AMD). *Immunol Lett*. 2012;147(1-2):29–33.
69. Niu N, Zhang J, McNutt MA. Endogenous IgG affects the cell biology of RPE cells and involves the TLR4 pathway. *Invest Ophthalmol Vis Sci*. 2013;54(10):7045–7052.
70. Loughland JR, Minigo G, Sarovich DS, et al. Plasmacytoid dendritic cells appear inactive during sub-microscopic Plasmodium falciparum blood-stage infection, yet retain their ability to respond to TLR stimulation. *Sci Rep*. 2017;7(1):2596.
71. Röck J, Schneider E, Grün JR, et al. CD303 (BDCA-2) signals in plasmacytoid dendritic cells via a BCR-like signalosome involving Syk, Slp65 and PLCgamma2. *Eur J Immunol*. 2007;37(12):3564–3575.
72. Dzionek A, Fuchs A, Schmidt P, et al. BDCA-2, BDCA-3, and BDCA-4: three markers for distinct subsets of dendritic cells in human peripheral blood. *J Immunol*. 2000;165(11):6037–6046.
73. Schuster P, Donhauser N, Pritschet K, et al. Co-ordinated regulation of plasmacytoid dendritic cell surface receptors upon stimulation with herpes simplex virus type 1. *Immunology*. 2010;129(2):234–247.
74. Heckenlively JR, Fawzi AA, Oversier J, Jordan BL, Aptsiauri N. Autoimmune retinopathy: patients with antirecoverin immunoreactivity and panretinal degeneration. *Arch Ophthalmol*. 2000;118(11):1525–1533.
75. Adamus G. Importance of autoimmune responses in progression of retinal degeneration initiated by gene mutations. *Front Med (Lausanne)*. 2021;8:672444.
76. Strong S, Liew G, Michaelides M. Retinitis pigmentosa-associated cystoid macular oedema: pathogenesis and avenues of intervention. *Br J Ophthalmol*. 2017;101(1):31–37.
77. Gong J, Cheung S, Fasso-Opie A, et al. The impact of inherited retinal diseases in the United States of America (US) and Canada from a cost-of-illness perspective. *Clin Ophthalmol*. 2021;15:2855–2866.
78. Ellingford JM, Barton S, Bhaskar S, et al. Molecular findings from 537 individuals with inherited retinal disease. *J Med Genet*. 2016;53(11):761–767.
79. Martin-Merida I, Avila-Fernandez A, Del Pozo-Valero M, et al. Genomic landscape of sporadic retinitis pigmentosa: findings from 877 Spanish cases. *Ophthalmology*. 2019;126(8):1181–1188.
80. Villanueva-Mendoza C, Tuson M, Apam-Garduño D, et al. The genetic landscape of inherited retinal diseases in a Mexican cohort: genes, mutations and phenotypes. *Genes (Basel)*. 2021;12(11):1824.
81. Cremers FPM, Boon CJF, Bujakowska K, Zeitz C. Special issue introduction: inherited retinal disease: novel candidate genes, genotype–phenotype correlations, and inheritance models. *Genes (Basel)*. 2018;9(4):215.
82. Iannaccone A, Radic MZ. Increased protein citrullination as a trigger for resident immune system activation, intraretinal inflammation, and promotion of anti-retinal autoimmunity: intersecting paths in retinal degenerations of potential therapeutic relevance. *Adv Exp Med Biol*. 2019;1185:175–179.
83. Yang P, Lockard R, Titus H, et al. Suppression of cGMP-dependent photoreceptor cytotoxicity with mycophenolate is neuroprotective in murine models of retinitis pigmentosa. *Invest Ophthalmol Vis Sci*. 2020;61(10):25.
84. Liu X, Feng B, Vats A, et al. Pharmacological clearance of misfolded rhodopsin for the treatment of RHO-associated retinitis pigmentosa. *FASEB J*. 2020;34(8):10146–10167.

Investigative Ophthalmology & Visual Science